Infrared fluorescence for vascular barrier breach *in vivo* – A novel method for quantitation of albumin efflux

Annette von Drygalski[1,2]; Christian Furlan-Freguia[3]; Laurent O. Mosnier[2]; Subramanian Yegneswaran[2]; Wolfram Ruf[3]; John H. Griffin[1,2]

[1]University of California San Diego, Department of Medicine, San Diego, California, USA; [2]The Scripps Research Institute, Department of Molecular and Experimental Medicine, La Jolla, California, USA; [3]The Scripps Research Institute, Department of Immunology and Microbial Science, La Jolla, California, USA

Summary

Vascular hyperpermeability contributes to morbidity in inflammation. Current methodologies for *in vivo* assessment of permeability based on extravasation of Evans Blue (EB)-bound albumin are cumbersome and often lack sensitivity. We developed a novel infrared fluorescence (IRF) methodology for measurement of EB-albumin extravasation to quantify vascular permeability in murine models. Vascular permeability induced by endotoxaemia was examined for all solid organs, brain, skin and peritoneum by IRF and the traditional absorbance-based measurement of EB in tissue extracts. Organ IRF increased linearly with increasing concentrations of intravenous EB (2.5–25 mg/kg). Tissue IRF was more sensitive for EB accumulation compared to the absorbance-based method. Accordingly, differences in vascular permeability and organ EB accumulation between lipopolysaccharide-treated and saline-treated mice were often significant when analysed by IRF-based detection but not by absorbance-based detection. EB was detected in all 353 organs analysed with IRF but only in 67% (239/353) of organs analysed by absorbance-based methodology, demonstrating improved sensitivity of EB detection in organs with IRF. In contrast, EB in plasma after EB administration was readily measured by both methods with high correlation between the two methods (n=116, r2=0.86). Quantitation of organ-specific EB-IRF differences due to endotoxin was optimal when IRF was compared between mice matched for weight, gender, and age, and with appropriate corrections for organ weight and EB plasma concentrations. Notably, EB-IRF methodology leaves organs intact for subsequent histopathology. In summary, EB-IRF is a novel, highly sensitive, rapid, and convenient method for the relative quantification of EB in intact organs of treatment versus control mice.

Keywords

Vascular permeability, endotoxaemia, method, lipopolysaccharide, Evans Blue

Correspondence to:
Annette von Drygalski, MD, Pharm D
The Scripps Research Institute
Department of Molecular and Experimental Medicine, MEM 180
10550 N. Torrey Pines Rd
La Jolla, CA 92037, USA
Tel.: +1 858 784 8220, Fax: +1 858 784 2243
E-mail: avondrygalski@ucsd.edu

Received: March 26, 2012
Accepted after major revision: August 28, 2012
Prepublished online: October 10, 2012
doi:10.1160/TH12-03-0196
Thromb Haemost 2012; 108: ■■■

Introduction

Injury resulting in hyperpermeability of the vascular endothelial barrier and consequent interstitial oedema is central to important mechanisms for organ dysfunction, organ failure, and death in sepsis (1, 2). However, while vascular leak seems to become increasingly central to our understanding of mechanistic contributions to pathophysiology and death in sepsis and other acute or chronic inflammatory conditions that affect cardiovascular and other diseases, precise quantification of vascular permeability as an endpoint in animal models is limited by current methodologies. Sepsis is the most deadly inflammatory disorder worldwide with mortality rates ranging from 30–70% when sepsis is severe (3). Compared to other disease entities, medical advances have been modest and today consist of prompt antibiotics, fluid resuscitation, and steroids. In part, the paucity of treatment options is due to our rudimentary understanding of the consequences of severe inflammation in the host, which includes vascular injury. Improved understanding of endothelial pathophysiology for mechanisms of vascular leakage, organ failure and death is therefore well warranted and could contribute to the development of vascular barrier therapeutics (1).

The development of modern methodologies to quantify vascular permeability has not kept pace. Vascular permeability in animal models of experimental inflammation is often based on measurement of albumin-bound Evans Blue (EB) extravasation into tissues and constitutes a highly relevant, physiological endpoint. However, measurement of EB in organs typically relies on a method that was developed in the 1950s for the quantitation of albumin distribution in mammalian tissues (4–6). It requires drying of tissues and organic solvent extraction for days followed by absorbance (620–659 nm) measurements of EB in extracts. Absorbance values have to be corrected for the presence of heme pigments (residual blood and, in the liver, bilirubin) that absorb at similar

wavelengths. The EB dye extracted from each organ has to be normalised to dry organ weight, which renders the organs unusable for further investigations (e.g. pathology or molecular studies). This is especially unfortunate if the number of animals available for each experiment is limited, as often is the case with genetically modified mice. Therefore, we developed a novel methodology employing near-infrared fluorescence (IRF) using the LI-COR Odyssey infrared Imager to quantify EB leakage in murine injury models. While fluorescence properties of EB are recognised, a method to quantify EB fluorescence in intact organs has not yet been described. This novel IRF-based method for EB detection permits reliable relative quantification of treatment-induced changes in albumin-bound EB in the extravascular compartment. To a first approximation, IRF differences reflect changes in vascular permeability; however, the method per se does not distinguish between changes due to organ/tissue damage, increased hydrostatic pressure, or other driving forces that push EB-albumin out of the blood vessels. Here, we will interpret IRF changes as due to vascular permeability while keeping these points in mind.

In this report, we describe our IRF-based methodology in detail with emphasis on its technical advantages and ease of application in a mouse model of lipopolysaccharide (LPS)-induced inflammation. This new IRF method is highly sensitive, quantitative, and fast with results available on the day of experimentation. Compared to absorbance-based measurements it leaves all solid organs intact for histopathology and other desirable analyses. Moreover, it allows accurate detection of relative changes within one organ system in EB-albumin vascular leakage with10– to 20-fold greater sensitivity compared to EB extraction. This novel method should facilitate assessment of EB-albumin leakage as an endpoint in many murine models of inflammation where endothelial damage and vascular permeability are pathogenic.

Material and methods

Animals

All animal protocols were carried out as approved by the institutional animal and care committee of The Scripps Research Institute. Mice were predominantly C57Bl/6J. In some experiments, PAR1$^{-/-}$ mice (7) or EPCR low mice (8) were used as indicated (generous gift from Francis Castellino, University of Notre Dame, Notre Dame, IN, USA).

LPS-injections

Mice, 6–8 weeks old, were injected intraperitoneally (i.p.) with LPS (5–8 mg/kg), (*E.coli serotype 0111:B4*; Calbiochem) or with equal volumes of 0.9% saline. LPS was solubilised in 0.9% sterile sodium chloride for injection by vortexing and sonication.

EB injections

At 18 hours (h) after LPS injection, weight-based injections of EB (Sigma) at 2.5, 5.0, 25 or 50 mg/kg in 0.9% sterile sodium chloride for injection were performed intravenously (i.v.) by lateral tail vein injection. Prior to injection, EB solutions were sterile-filtered (Millex®, 0.22 μm; Millipore).

Blood and organ harvest

For determination of peak plasma values of EB, retro-orbital bleeds were performed 2 minutes (min) after EB injection and 75 μl of blood was drawn into heparin-coated microcapillaries (Fisher Scientific, Waltham, MA, USA). At 30 or 45 min after EB injection, mice were anesthetised and, the abdominal cavity and chest were opened by blunt dissection. The vena cava was visualised and severed below the renal vessels. Organs were flushed gently with a total of 40 ml saline by inserting a 22-gauge needle first into the right heart and then into the left heart, thereby removing EB dye from vasculature in the lungs and other organs, followed by organ harvest.

Simultaneous determination of EB in plasma by IRF and absorbance spectrophotometry

Blood samples after i.v. injection of EB were flushed from microcapillaries into Eppendorf tubes (USA Scientific, Ocala, FL, USA) with 200 μl of saline (final total volume 275 μl). The diluted blood was spun at 3,000 rpm for 10 min, and 150 μl of the diluted plasma supernatant was removed from each sample and added to 200 μl of saline into 48-well tissue culture plates (Costar®, Corning Inc., Corning, NY, USA). This provided an 8.5-fold dilution of plasma EB which proved optimal for detection by IRF as well as absorbance. Plates were first subjected to IRF methodology on the Odyssey infrared imager (LI-COR, Lincoln, NE, USA), 700 channel with focal plane set at 4 mm and laser intensities set at 3.5–4.5. Area intensities from the bottom of each well were recorded as integrated fluorescence intensities (I.I.) per well area. After completion of IRF measurements, 200 μl were withdrawn from each well, added to 96-well flat bottom assay plates (Costar®) and EB in plasma was measured by absorbance spectrophotometry at 620 nm and 740 nm (Optimax Microplate Reader; Molecular Devices). Values were expressed as optical density (OD) and corrected for hemoglobin with the following formula: OD620-(1.426xOD740+0.03) (9, 10).

EB detection in organs by IRF methodology

EB IRF was performed using the Odyssey infrared imager (LI-COR) with Application software version 3.0 using the 700 channel

(excitation by solid-state diode laser at 685 nm and emission 700–750) with the focal plane of the microscope head set at 1 mm. Freshly harvested organs were weighed and, dependent on organ size, placed on the inner surface of lids from 6-, 12– or 24-tissue culture plates (Costar®). Organs with flat surfaces (skin, peritoneum, liver, lung, brain) were left intact, while small round or cubic shaped organs (heart, spleen, kidney) were cut in half and pressed gently onto the plastic surface. Each organ system was scanned separately using the Odyssey. Laser intensities for the organ system were chosen based on an optimal linear range of fluorescence intensities. After scanning, organ shapes were encircled by the automated drawing tool provided with LI-COR analysis software and fluorescence intensity captured over the encircled organ area was recorded as raw fluorescence intensities (designated RFI per manufacturer).

Quantitation of EB in organs following IRF methodology

Two approaches for quantitative determination of EB with IRF in organs are possible for flexibility dependent on experimental design and objectives. First, RFI was divided by dry organ weight in analogy to the traditional absorbance-based EB detection method where EB content in extracts is divided by dry organ weight. However, EB quantitation by IRF in fresh organs *per* weight may be inaccurate, if experimental conditions lead to volume shifts, organ expansion, and/or if mice vary in weight and organ sizes.

The preferred approach for IRF quantitation in fresh organs is therefore multiplication of RFI by organ weight. The rationale to multiply rather than divide by weight is inherent to the RFI methodology where EB is determined in a "slice" of the organ and not the whole organ. It is important to note that RFI is an estimation of the EB concentration in the organ and not a determination of the total EB amount in the organ. Thus to extrapolate the EB in the "slice" to the whole organ, one would have to add the number of "slices" in the organ (or multiply by weight). This approach relies on the assumption that RFI obtained at a certain "slice" of the organ is proportional to the total RFI in the whole organ, and thus assuming that the heterogeneity of EB distribution on the x-y dimension is proportional to the heterogeneity of the EB distribution in the y-z dimentsion. This approach should be most accurate if animals are well matched for gender, age and weight (≤ ± 5% of

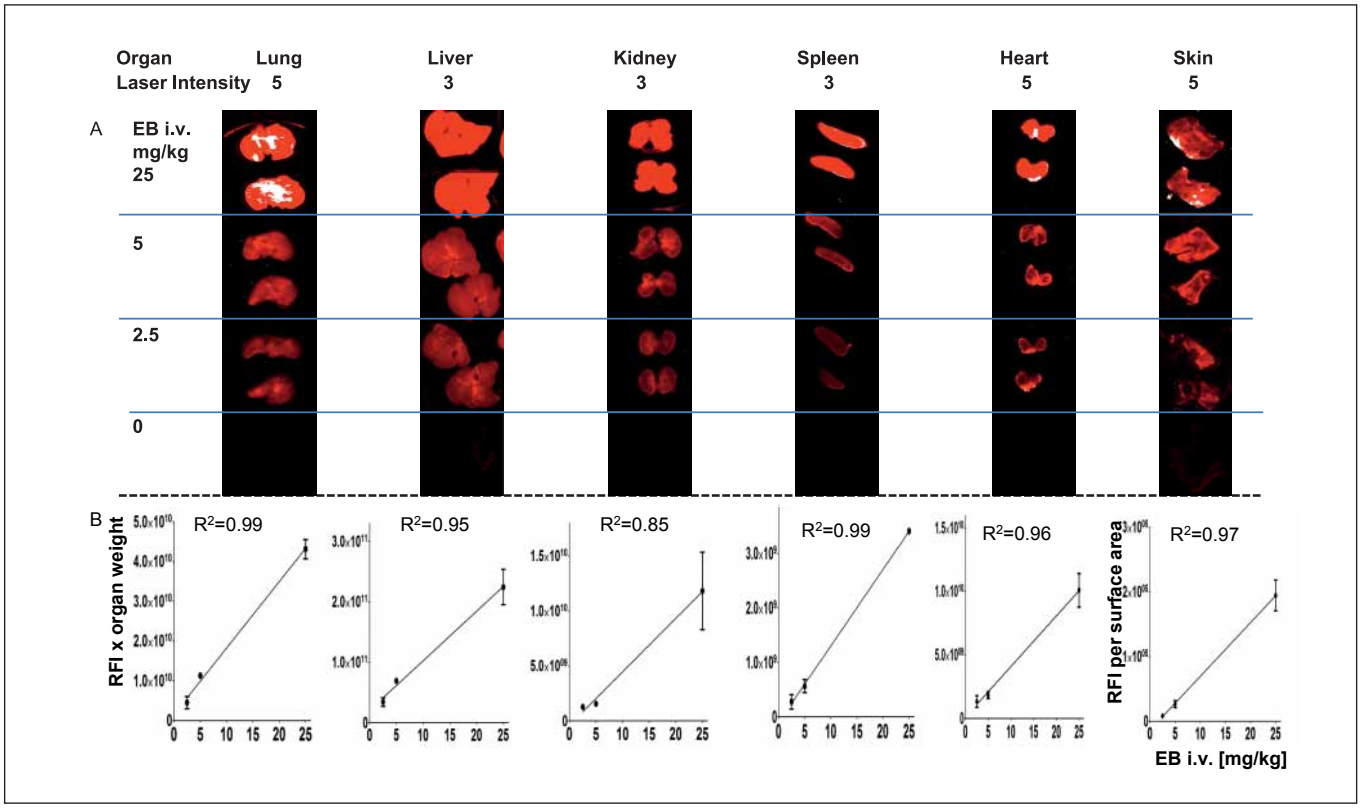

Figure 1: Increasing concentrations of i.v. EB yielded linear increase in organ IRF. C57Bl/6J mice were injected i.v. with 0, 2.5, 5 or 25 mg/kg EB. Organs were harvested 45 min later after organ flushing. A) Organ IRF yielded RFI values for each organ well above the no-EB background. RFI were normalised by multiplication with organ wet weight. For skin, RFIs were divided by shape surface area (RFI/mm^2). Laser intensity for each organ system was adjusted to best dynamic range. B) Increase in organ RFI signal was linearly proportional to EB dose injected. Curves were fit by linear regression analysis. For goodness of fit, all R^2 values are displayed (all $p \leq 0.01$ for difference from zero).

weight difference), such that equal organ volumes and sizes are likely at baseline. If complicated volume shifts occur under experimental conditions, such as through dehydration and/or plasma extravasation into organs, total EB dye accumulation in an organ can be directly compared to total EB dye organ accumulation in the same organ of another animal. Since fluorescence intensity was recorded as raw fluorescence intensity without correction for the surface area of the organ to minimise introduction of additional bias, the current method is intended to compare IRF within the same organ system of treated versus control mice but does not permit for the direct comparison of IRF between one organ system to another.

In addition, to achieve even greater precision, RFI obtained in wet organs as described above was divided by peak plasma RFI briefly after EB injection, thus correcting for minor volume variations when injecting EB in experimental reality, and potentially for changes in EB clearance (see ▶Suppl. Fig. 1 for details, available online at www.thrombosis-online.com).

For thin layers of tissue (such as skin or peritoneum) RFI were quantified relative to surface area (RFI/mm^2) without corrections for organ weight.

EB detection in organs by the absorbance-based method

After IRF measurements, EB in organs was determined using the traditional absorbance-based method. Organs were dried overnight at 60°C, weighed, crushed and incubated in defined volumes of formamide (250–1000 µl depending on organ size) for three days at 25°C. Organ extracts were centrifuged at 3,000 rpm for 10 min to remove particulate matter. Two hundred µl of the supernatants were added to 96-well flat bottom assay plates (Costar®). Absorbance of EB was measured at 620 and 740 nm (Optimax Microplate Reader; Molecular Devices, Sunnyvale, CA, USA). Values were corrected for hemoglobin (OD620-(1.426xOD740+0.03) (9;10) and expressed as OD per gram organ dry weight.

Histology

Following IRF measurements, fresh tissues were placed in $ZnSO_4$-buffered 10% formalin and processed routinely, embedded

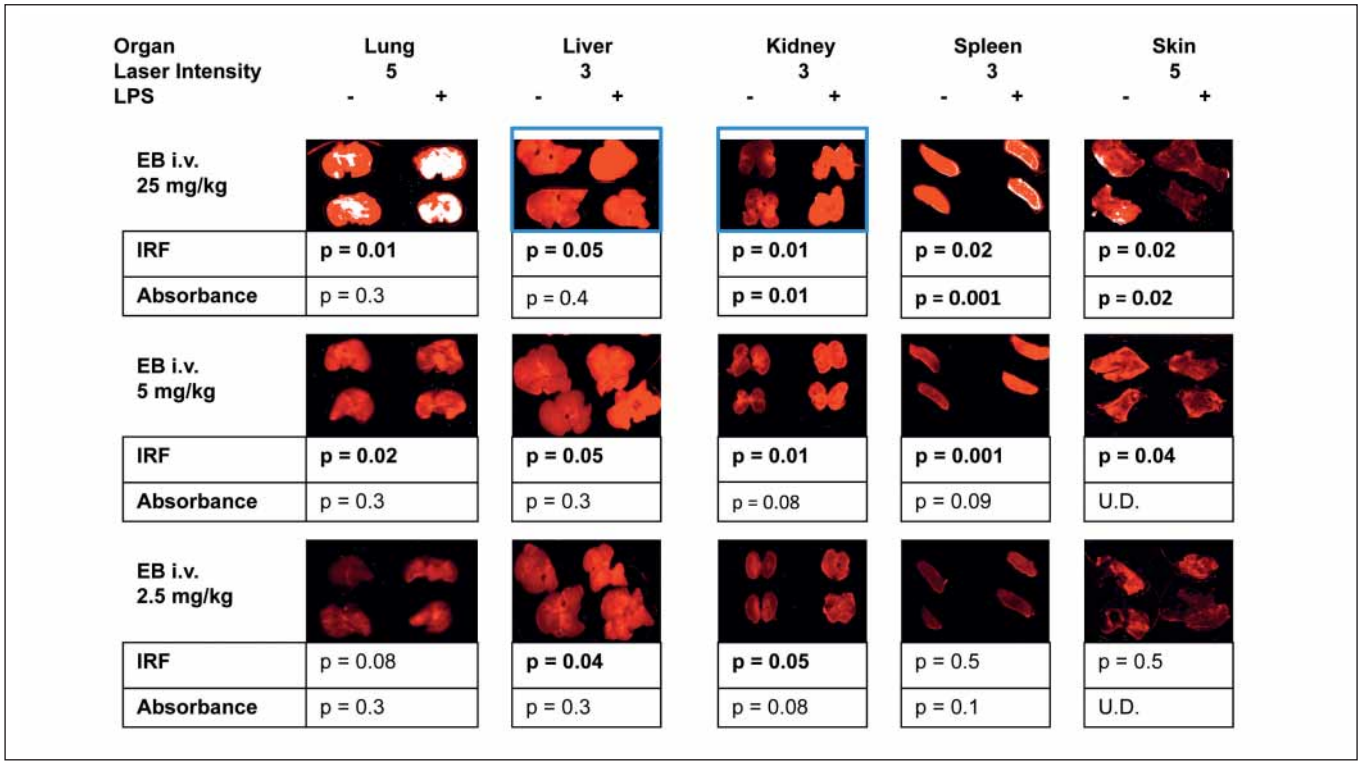

Figure 2: Improved sensitivity of organ EB detection by IRF compared to the absorbance-based method. C57BL/6J mice were injected with LPS (5 mg/kg i.p) or saline (n=12). Doses of EB (25, 5 and 2.5 mg/kg) were injected i.v. .EB in fresh organs was quantified by IRF multiplied by wet weight, and for skin per surface area in mm^2. Subsequently, EB organ accumulation was determined for the same organs after formamide extraction and EB detection by absorbance divided by dry weight (as this is standard for absorbance-based method). In contrast to EB detection by absorbance, IRF revealed significantly higher sensitivity for detection of significant ($p \leq 0.05$) differences in EB accumulation between organs of untreated and LPS-treated mice at all EB dose levels. Blue frames indicate manual modulation of gamma-values for better visualisation of differences. This had no effect on the pixel intensity values used for RFI quantitation. Absolute measurements are shown in Suppl. Figure 2 (available online at www.thrombosis-online.com). U.D., undetectable.

in paraffin, sectioned at 3 micron, and stained with hematoxylin and eosin (H/E).

Determination of hemoglobin fluorescence

Haemoglobin (human, No.H-7379; 2x crystallised, Sigma, St. Louis, MO, USA), was reconstituted in 0.9% saline at 12 g/dl (physiological concentration in blood) and scanned on the Odyssey (LI-COR) in 7 serial 1:1 dilutions in 96 well plates in the 700 channel with focal plane set at 4 mm and laser intensity set at 5.

Statistical analysis

Student's t test, Pearson correlation coefficient (r^2), McNemar test for binary variables and linear regression analysis were used to assess statistical significance where appropriate. Depending on the test, p-values of ≤0.05 and/or 95% confidence intervals (CI) provided statistical significance.

Results

Detection limit and sensitivity of EB quantitation in organs for IRF- and absorbance-based methods

The dose range of i.v. EB currently used for detection of EB in tissues using absorbance-based detection is 20–50 mg/kg (11–14). Since 50 mg/kg EB i.v. yielded signal saturation of IRF in most organs at the lowest laser intensities (data not shown), we chose 25 mg/kg EB i.v. as the upper dose limit for IRF and injected doses of 25, 5 and 2.5 mg/kg into C57Bl/6J mice. For each dose, mice (n=6; weight matched) were injected, and after 45 min, organs were harvested, followed by IRF determination of EB in fresh organs (lung, liver, kidney, spleen, heart, skin). For solid organs RFI were multiplied by wet weight. For skin (thin tissue layer), RFI were divided by surface area). EB fluorescence was detectable at all dose levels of EB, even at 2.5 mg/kg, which is 10– to 20-fold less than the EB dose usually necessary for detection with absorbance spectrophotometry. The increase in IRF in all organ systems was proportional to the EB dose injected (▶Fig. 1) which showed the extended sensitivity of IRF for the detection of EB. It also revealed that blood perfusion and tissue exchange of albumin create concentration dependent baseline tissue levels of EB that will not be removed by systemic flushing of organs. Therefore, the sensitivity of the EB detection method is useful for quantifying vascular permeability changes over baseline in experimental settings.

To demonstrate that EB tissue detection with IRF is superior to absorbance spectrophotometry for the discrimination of incremental changes in organs under experimental conditions, we simultaneously challenged a second group of C57Bl/6J mice (n=6; weight matched) with LPS (5 mg/kg i.p.). EB injections, determinations of EB organ accumulation by IRF as well as by absorbance measurements were carried out in parallel for the untreated and LPS-treated mice at all three dose levels of i.v. EB. The results obtained with both methods were compared directly for individual organ systems (▶Fig. 2). With IRF (multiplication of RFI by organ wet weight), differences in EB organ accumulation between untreated and LPS-treated mice were visually recognisable at all three dose levels of i.v. EB (▶Fig. 2). EB accumulation after LPS was increased in lung, liver, kidney, spleen and decreased in the skin. No differences in EB accumulation were found for the heart (data not shown). This pattern of EB organ distribution may have mirrored perfusion physiology in shock, where central blood pooling (+/- exudation) occurs at the expense of peripheral vasoconstriction. At 25 mg/kg i.v. EB, IRF detected a significant difference (p≤0.05) between LPS-treated and non-treated mice in all five organs analysed, whereas the traditional absorbance-based method only detected significant differences in three out of five organs, but not in lung and liver, two organs that are very relevant to vascular permeability studies (see ▶Suppl. Fig. 2, available online at www.thrombosis-online.com). Using the IRF detection method for EB, these differences between organs of LPS-treated and non-treated mice were reproduced when EB concentrations were five-fold lower (5 mg/kg EB i.v.). Remarkably, the traditional absorbance-based method failed to detect any significant differences at 5 mg/kg EB i.v. regardless of the organ studied. Even at 2.5 mg/kg EB i.v significant differences between liver and kidney of LPS-treated and non-treated mice could be observed using the IRF methods. Overall, in efforts to detect endotoxin-induced changes in vascular permeability in individual organ systems, IRF yielded significant differences in 11/15 instances, whereas absorbance-based detection of EB did so in only 3/15 instances (p=0.02; McNemar test) (▶Fig. 2). These results clearly illustrate the benefit of increased sensitivity of EB detection for the determination of vascular permeability *in vivo*. In addition, increased sensitivity of EB detection permits the use of lower concentrations of EB in the circulation reducing the risk of confounding EB-induced vascular effects that have been reported to occur at EB concentrations of 50 mg/kg and above (4).

Validation of IRF methodology for EB detection in fluids

To validate IRF as an appropriate method to detect EB in bodily fluids, we compared IRF methodology directly with absorbance-based detection of EB in plasma samples of mice following EB injection. Following i.v. injection of EB, plasma is the compartment with the highest EB concentration and, therefore, EB detection by absorbance was not hampered by its detection limits. Plasma samples were drawn from 58 mice, at 2 min and at 30 or 45 min (total 116 samples) after i.v. injection of EB (25 mg/kg). Mice were either C57Bl/6J (n=20) or EPCR low (n=38) and were treated either with LPS (n=36) or saline (n=22) prior to EB injection. Samples were processed as outlined in *Materials and methods*. In all

circumstances, highly significant correlations were found between EB concentrations determined by IRF versus absorbance (▶Fig. 3). Thus, IRF methodology is highly suitable for EB plasma concentration measurements.

Direct comparison of IRF and absorbance methodologies for EB quantitation in individual organ systems

With the EB detection method by IRF validated in plasma samples, we next optimised EB detection in tissues using IRF and compared the results in various individual organ systems (kidney, lung, peritoneum, heart, spleen, liver, brain) directly to those obtained using the absorbance-based method. The purpose was to confirm the previously observed (▶Fig. 2) higher sensitivity of detection of EB with IRF methodology in a larger series of experiments, and to demonstrate that IRF measurements of EB content in fresh wet organs can replace methodology requiring dry weight normalisation. Immediate wet weight determination of EB would provide important methodical improvement regarding labour, procedural length and utilisation of fresh organs for further studies. Mice (57 in total; C57 Bl/6J, n= 22; PAR-1$^{-/-}$, n=4; EPCR low, n=31) received LPS (5–8 mg; i.p.; n=37) or saline (n=20) prior to i.v. EB (25 mg/kg). Organ IRF was normalised to wet weight (RFI multiplied by fresh organ weight) or to dry weight (RFI divided by dry organ weight), and both those modalities were compared to the absorbance-based method, where ODs in extracts from the same organs were divided by dry weight.

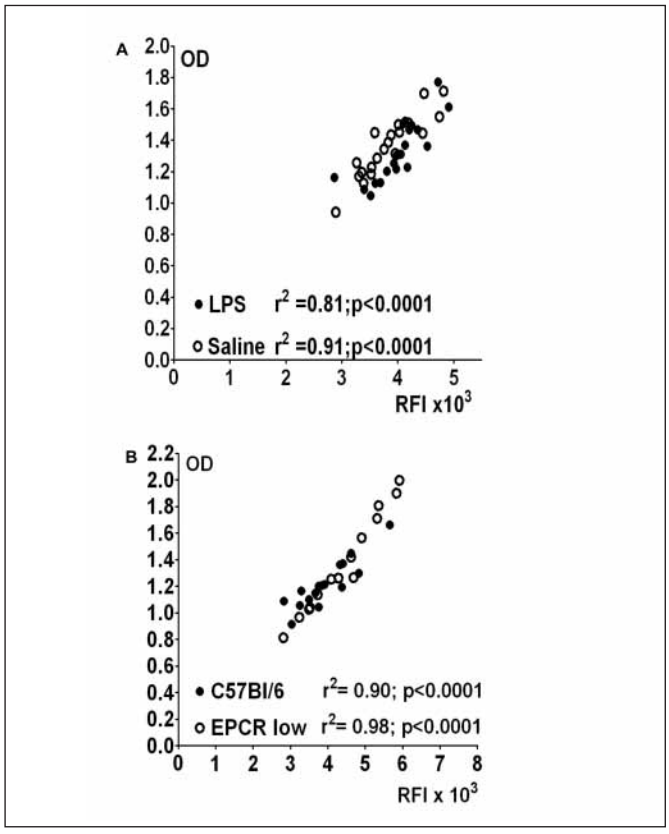

Figure 3: Significant correlation of EB in plasma determined by IRF- and absorbance-based methods. Mice were injected with i.v. EB at 25 mg/kg 18 h after receiving LPS (5–8 mg/kg; i.p.) or saline. EB plasma concentrations for each mouse were determined at 2 and 30 or 45 min after EB injection. EB plasma concentrations were measured by IRF (RFI on X-axis) and by absorbance (OD on Y-axis). Correlations between methods were determined by Pearson correlation coefficient (r^2). A) Correlations of EB values in samples from C57Bl/6J mice injected with saline (n=20) or LPS (n=20) detected with both methods were highly significant. B) Representative example of results of an experiment depicting highly significant correlations of EB values determined with both methods for blood samples from LPS-injected C57Bl/6J (n=14) or EPCR low mice (n=14).

The sensitivity of the IRF methodology for EB detection in organs was significantly better compared to the absorbance-based method. While IRF provided EB values for 353/353 organs tested (100%), detection of EB above background using absorbance was successful for only 230/353 organs tested (65%). Using absorbance to determine EB levels in organs, percent successful detection with was highest for kidney (100%) and peritoneum (100%), whereas EB determinations in lungs, heart, liver, spleen and brain was only possible in 82%, 70%, 59%, 58% and 7% of organs, respectively (▶Fig. 4). Despite the unreliable detection of EB in a large subset of the organs examined using the absorbance-based method, in those instances where tissue EB could be quantified, values correlated well with values obtained by IRF for all organs examined when both methods were normalised to dry organ weight (division of RFI by dry weight) (data not shown).

As one of the perceived benefits of the IRF methodology is the preservation of the organs for subsequent histopathological analysis, we determined whether normalisation of RFI to fresh organ weight (multiplication of RFI by wet weight) rather than dry weight (division of RFI by dry weight) was possible. The rationale for normalisation of RFI to fresh organ weight using multiplication of RFI by wet weight rather than division of RFI by wet weight is described in the methods section. Correlations of IRF by wet weight with Absorbance by dry weight or of IRF by dry weight with Absorbance by dry weight yielded similar results for individual organs. Also, no statistically significant differences were found between the means of correlation coefficients derived from all organ systems with IRF normalised to dry weight (0.86; SEM 0.02; n=29) or wet weight (0.82; SEM 0.02; n= 29).

Taken together, these results indicate that EB organ detection with IRF methodology of fresh tissue (multiplication of RFI by wet weight) has higher sensitivity than detection of EB by absorbance, and is non-inferior and feasible compared to approaches employing dried tissue (traditional EB quantitation by absorbance).

IRF methodology for EB detection in peritoneum and skin

For peritoneal surfaces, which may be of interest in models of mesenterial inflammation, detection of EB was very good with both

methods (▶Fig. 4). As opposed to other organs, the thin and membranous tissue structure of peritoneum seems to permit easy formamide extraction of EB in sufficient quantities for absorbance measurements.

IRF methodology can provide accurate results of EB quantitation in hairy fresh skin by quantifying fluorescence by surface area rather than weight. Quantitation relative to surface area yielded linearity of IRF after i.v. injection of increasing doses of EB (2.5, 5 and 25 mg/kg) (▶Fig. 1). We did not study EB accumulation in skin by absorbance spectrophotometry since it requires prior hair shaving, with added length of anesthesia and stress to animals. Loose hair in formamide is difficult to pellet in small volumes and will interference with absorbance measurements.

EB quantification in organs with IRF methodology was reproducible in a mouse model of inflammation

To demonstrate that IRF methodology for EB quantification in tissues is applicable to experimental inflammation, we injected either LPS (8 mg/kg i.p.) or saline into two groups of weight-matched female C57Bl/6J mice. Two independent experiments were carried out (n=5 mice per group; total n=20). Injection of LPS or saline was followed by i.v. EB (25 mg/kg) at 18 h, followed by organ harvest after either 30 or 45 min and subsequent IRF quantitation (RFI multiplication by wet weight). To increase precision of EB quantitation in organs, values were corrected for EB plasma fluorescence given that increasing concentrations of circulating EB had resulted in a linear increase of EB IRF in organs (▶Fig. 1) and variations in plasma EB levels despite EB dosing per weight (▶Fig. 3). In experimental reality, despite weight-based injections, mild variations of EB plasma levels in individual mice were unavoidable. While those variations may not appear statistically significant, they may still influence EB tissue quantitation as illustrated in ▶Suppl. Figure 1 (available online at www.thrombosis-online.com) for one pair of matched mice that belonged to the LPS- and saline-injected groups of animals. Although there was no statistically significant difference in mean EB plasma fluorescence between the two groups injected with LPS or saline (mean RFI 4309 (SEM 100) vs. 4150 (SEM 150); p=0.5), the individual values of these two mice were the highest (4900 RFI; LPS-group) and lowest (3400; saline group) within their respective groups. Since the differences in plasma fluorescence would influence baseline organ fluorescence, we corrected each mouse's organ fluorescence (normalised to wet weight) by its peak plasma fluorescence (drawn 2 min after EB injection). By forming this ratio, EB tissue IRF in the LPS-treated mouse became attenuated while EB tissue IRF in the saline-mouse increased. Only the difference between those ratios accurately reflects the increase in EB tissue accumulation caused by LPS. Thus, irrespective of the method used, determining accurate quantitative differences of EB organ accumulation between experimental groups of animals requires correction based on EB plasma levels (15).

With EB plasma correction implemented, EB was quantified in

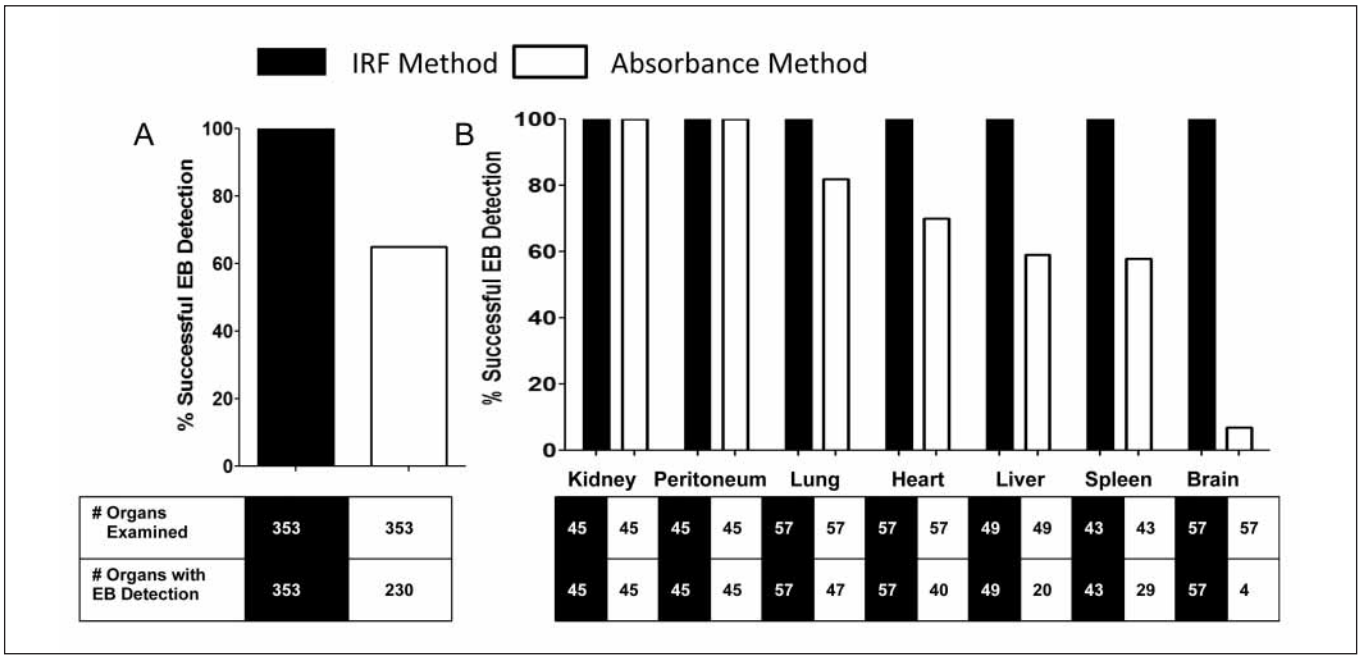

Figure 4: Quantification success of EB in organs: Direct comparison of IRF- and absorbance-based methodologies. EB accumulation was assessed in organs of mice (C57Bl/6J; PAR1$^{-/-}$; EPCR$_{low}$), some of which had been injected with LPS (5–8 mg/kg i.p.) 18 h prior to i.v. EB (25 mg/kg) and organ harvest. EB accumulation was determined in fresh organs by IRF methodology, and subsequently by the absorbance method. A) Success rate of EB detection above the detection limit in the total number of organs studied using both methodologies. B) Success rate of EB detection above the detection limit classified for each organ system studied using both methodologies.

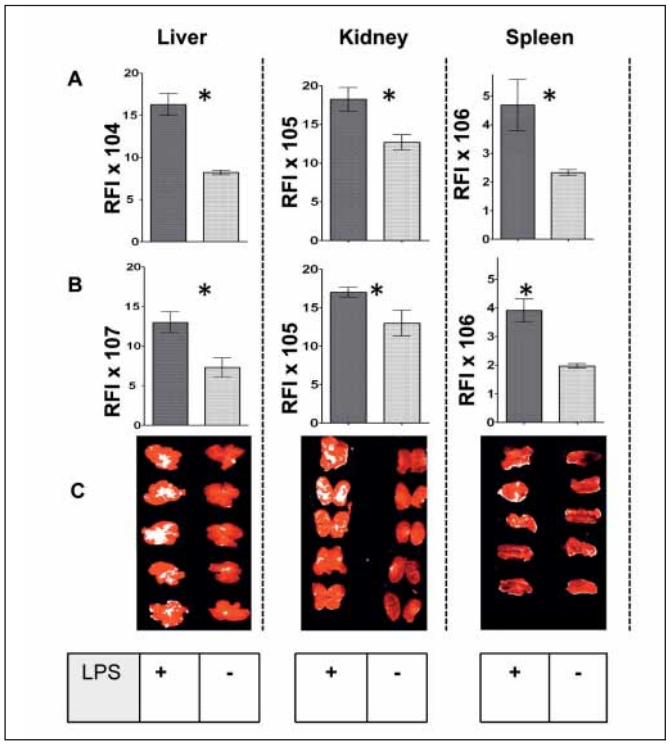

Figure 5: EB accumulation quantified by IRF in liver, kidney and spleen is significantly increased in LPS-injected mice. C57Bl/6J mice were injected with LPS (8 mg/kg i.p) or an equal volume of saline (n=5 per group). At 18 hours, EB (25 mg/kg, i.v.) was given and organs were then harvested after 45 min (A) or 30 min (B). RFIs were multiplied by fresh organ wet weight and divided by peak plasma RFI. EB IRF was significantly increased in livers, kidneys and spleens of LPS-injected mice compared to saline-injected mice (* p≤0.05). C) Organs from one representative set of experiments are shown as visualised on the Odyssey.

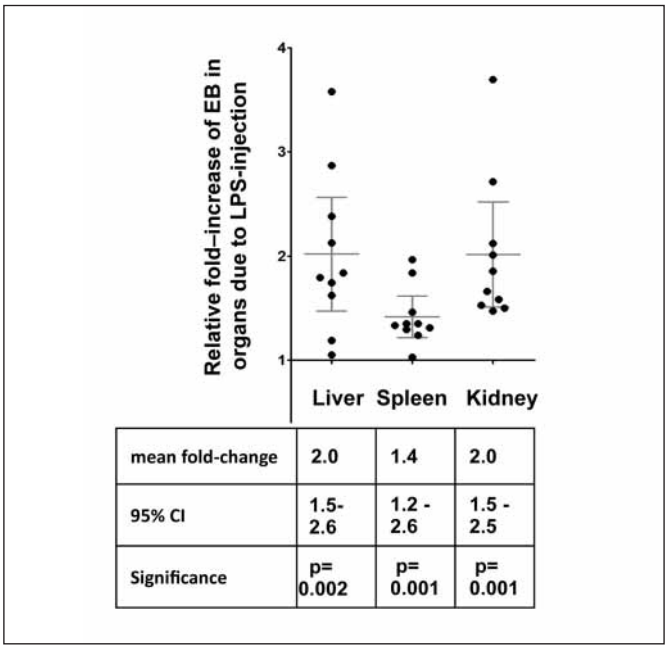

	Liver	Spleen	Kidney
mean fold-change	2.0	1.4	2.0
95% CI	1.5-2.6	1.2 - 2.6	1.5 - 2.5
Significance	p= 0.002	p= 0.001	p= 0.001

Figure 6: Relative increase of EB accumulation in organs of LPS-injected mice compared to saline-injected control mice. Using age, weight and sex matched pairs of mice for LPS and saline-controls, RFI for EB fluorescence in the organ of an LPS-injected mouse was directly compared to its matched control at 18 h after endotoxin treatment and expressed as a relative ratio EB increase (Y-axis: 1= no difference). Organ RFI was obtained by multiplication of RFI with wet weight, divided by peak plasma RFI. Student t-test was used for analyses. Error bars correspond to 95% CI.

fresh organs of 20 LPS-treated or saline-treated mice. LPS-injected mice demonstrated significantly increased EB accumulation in livers, kidneys and spleens compared to saline-injected mice (▶Fig. 5). To address some of the complicated volume shifts that occur under experimental conditions age, sex- and weight-matched pairs of mice for LPS versus saline treatment were used based on the assumption that these pairs of mice will have a similar organ volumes at baseline. Using age, sex and weight matched pairs of mice for LPS versus saline treatment, permitted expression of the results for each pair of mice as relative change of EB fluorescence in the organ of an LPS-injected mouse compared to its matched control (n=10 pairs; ▶Fig. 6). A value of 1 indicates no relative difference due to LPS treatment. The mean increase of EB accumulation in LPS-injected over saline-injected mice was 2.0-fold (CI 1.5–2.6) for liver, 1.4-fold (CI 1.2–2.6) for spleen and 2.0-fold (CI 1.5–2.5) for kidney (all p <0.002). For lung, heart and brain, EB organ accumulation was similar, and no significant differences were present with mean relative changes for LPS-injected over saline-injected mice of 0.9-fold (CI = 0.7–1.1), 1.1-fold (CI = 0.9–1.2) and 1.1-fold (CI = 0.9–1.3), respectively (data not shown).

Expression of EB organ accumulation as relative increase or decrease between groups of animals facilitates data pooling from different experiments where different laser intensities were used engendering different absolute values for RFI. However, proportions of differences in repetitive experiments should remain the same and can therefore be expressed in relative terms of changes in RFI for comparisons among groups of animals.

Quantitation of EB by IRF methodology in fresh organs permits subsequent histological tissue examination and comparisons to tissue damage

After EB organ quantitation with IRF in mice injected either with LPS or saline as described above, fresh livers and lungs were submitted for histology. Tissue quality remained excellent and revealed focal areas of necrosis with infiltration of polymorphic mononuclear white cells in livers of the LPS-injected, but not of the saline-injected mice (▶Fig. 7). These areas corresponded to areas of EB leakage as visualised by naked eye and areas of saturated IRF on the Odyssey images (see also ▶Figs. 1, 2 and 5).

Of note, there was no significant increase in EB accumulation in lung tissue compared to saline, when 8 mg/kg LPS was injected, in contrast to injection of 5 mg/kg LPS (▶Fig. 1), for reasons that re-

main unclear. Interestingly, lung histology also did not differ between LPS-injected and saline-injected mice (see ▶Suppl. Fig. 3, available online at www.thrombosis-online.com). However, since tracheal formalin instillation or insufflation was not employed, we may have missed subtle findings suggestive of injury, inflammation or airway exudates in atelectatic areas. Nevertheless, the normal looking lung tissue correlated well with the fact that EB accumulation by IRF methodology was similar in both groups of mice. Therefore, as exemplified here with liver and lung, the magnitude of EB accumulation in tissues reflected the presence or absence of pathological findings. The results of these studies demonstrate that EB tissue accumulation varies with the degree of tissue or vascular barrier injury and can be sensitively quantified with IRF. Procedures during IRF scanning did not affect tissue integrity, thus allowing subsequent multi-purpose use of fresh tissues.

Fluorescence spectrum of hemoglobin does not interfere with IRF EB quantification

When haemoglobin fluorescence was determined on the Odyssey (LI-COR), no fluorescence was detected in the 700 channel (laser intensity 5) at the physiological concentration in blood (12 g/dl), demonstrating that haemoglobin does not interfere with EB fluorescence in the near-infrared region (see ▶Suppl. Fig. 4, available online at www.thrombosis-online.com).

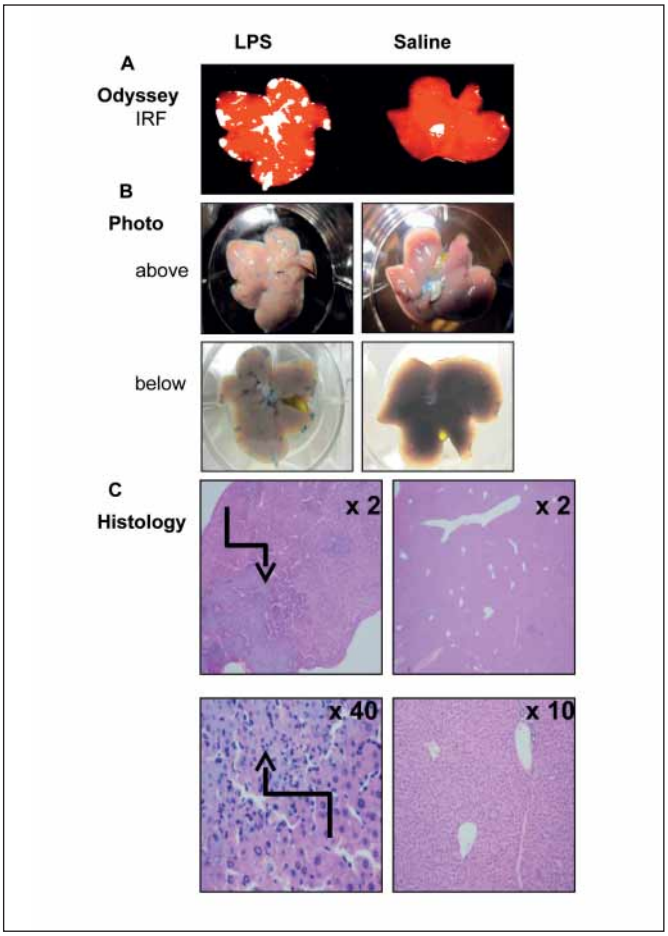

Figure 7: Quantitation of EB by IRF in fresh organs permits subsequent histological tissue examination. C57Bl/6J mice were injected i.p. with LPS (8 mg/kg) or saline and sacrificed 18 h later, 30 min after i.v. EB (25 mg/kg). A) EB accumulation in the liver, visualised with IRF for a representative pair of mice. B) Visual inspection revealed circumscribed areas of EB extravasation which corresponded to saturated (white) IRF in livers of LPS-treated mice. C) Following H/E staining, liver from LPS-treated mice revealed focal necrosis with infiltration of polymorphic mononuclear cells (black arrows), whereas livers of mice treated with saline were unremarkable. In the liver, focal areas of EB accumulation corresponded to histological areas of focal necrosis.

Discussion

Vascular leakage and edema are major contributors to pathogenesis and mortality in acute inflammatory conditions. *In vitro* studies of endothelial cell layer permeability have advanced knowledge about molecular pathways, but *in vivo* proof of concept studies of hyperpermeability are limited by absence of convenient and sensitive methodology (1). Near IFR analysis is ideal for biological tissue imaging because of minimal auto-fluorescence (16). Making use of EB's fluorescent properties in the near-infrared spectrum, we developed and validated a novel approach for quantitation of albumin extravasation and vascular barrier break in mice using the LI-COR Odyssey infrared imager. Applying IFR fluorescence to the physiological concept of tissue extravasation of albumin-bound EB resulted in several significant advantages over the traditional determination of EB in tissue extracts using absorbance measurements. Notably, the new method was superior in direct comparisons with the traditional absorbance-based method with regards to sensitivity of EB detection. Data here show that IRF quantitation of extravasation of albumin-bound EB, reflecting relative changes in vascular permeability, can be successfully applied to all solid organs as well as to brain, skin and peritoneal surfaces.

In a mouse model of endotoxaemia and acute inflammation, distinct and significant differences in tissue EB between LPS- and saline-treated mice could be detected with IRF methodology at i.v. doses of EB that were 10–20 times lower than the minimum required for the absorbance-based method. EB can affect blood pressure and pulse rate in small animals at doses of 50–100 mg/kg (4), which is the minimum dose range required for detection of extravasation by traditional absorbance-based methods for EB. Therefore, lower doses of EB injection using high sensitivity IRF methodology will improve precision of quantification of dye extravasation and, offers a significant advancement.

IRF allowed relative quantitation of EB in fresh organs with uncompromised subsequent histological tissue analysis. In contrast, methodology using EB detection by absorbance requires heme corrections and renders tissues unusable for further biological

analyses because of drying and formamide extraction. Moreover, histological tissue analyses after albumin-bound EB tissue extravasation quantified by IRF confirmed that EB accumulation corresponded to the presence of tissue injury, thereby saving time, labour, and animals.

The current IRF method was designed and validated for comparison of relative changes in EB extravasation in a particular organ system between mice receiving treatment versus control. An important methodological difference between the IRF method and the absorbance method is that IRF determines the concentration of EB in a "slice" of the organ and not the total amount of EB in the organ as with the absorbance method. Thus, the assumption that the RFI measured in the "slice" is proportional to the EB concentration in the organ is critical. Our data strongly supports this assumption because ▶ Figure 1 shows a linear correlation between EB concentration injected i.v. and RFI measured in organs and ▶ Figure 3 shows a linear correlation between plasma EB concentration and RFI measured. Furthermore, a significant correlation (r=0.82) between EB detection by absorbance (where organ extracted EB is divided by dry weight) and by IRF (where organ RFI are multiplied by wet weight) was found, indicating EB concentration in the "slice" multiplied by the wet weight of the organ is a valid estimate of the total EB in the organ. However, the current IRF methodology also holds limitations. The experimental setup employed here does not permit direct comparison of IRF values of one organ system to another. Future studies will have to evaluate to possibility to obtain absolute EB values from RFI to permit direct comparison of one organ system to another.

For physiological relevance, it has been long recognised that the principle of *in vivo* labelling of albumin with EB following its i.v. injection is advantageous. Once vascular integrity is compromised, albumin leak and the associated osmotic fluid efflux rapidly increase interstitial tissue pressures, both of which have emerged as major contributors to organ failure and death (1, 2). To assess vascular integrity, injection of small volumes of EB (≤100 µl) binding to circulating albumin is favourable. Exogenous, labeled (radioactive or fluorescent) albumin at larger volumes can invoke volume overload or species-related allergic reactions since murine albumin is not readily available. Similarly, while methods using labelled dextrans or polyethyleneglycol may be appropriate for some experimental settings (17), they could exhibit osmotic properties, changing vascular flow and volume dynamics.

EB methodology, initially developed in the 1950s for assessment of physiological albumin tissue distribution in mammals (4–6) became attractive for lung injury models in the 1980s-1990s, where EB could be quantified directly in lavage fluids and tissue extracts of larger organs (18–21). In addition, albumin-bound EB uptake into injured cardiomyocytes or neurons and subsequent quantitation by fluorescence microscopy has been exploited for cardiac and brain reperfusion after injury (22, 23). Over the past decade, there have been many attempts to optimise the EB methodology to solid organs in murine models of experimental inflammation with limited successful improvements. Solid tissue consistency and small organ volumes are a disadvantage if procedures like EB formamide extraction are necessary prior to EB detection by absorbance. Limitation in methodology for *in vivo* quantification of EB-albumin leakage in mice may explain why over the last decade little progress has been made in advancing knowledge about *in vivo* mechanisms for vascular leakage and clarification of its role for organ failure and death in small animal models of inflammation. In fact, the stimulus to develop this new IRF-based method was driven by our inability to study the biology of barrier stabilisation and the prevention of vascular leak through the actions of activated protein C and its receptors in endotoxaemia.

In summary, IRF methodology of extravascular albumin-bound EB in organs in murine injury models permits relatively rapid and convenient quantification of vascular permeability changes within a particular organ system with increased sensitivity relative to traditional absorbance-based methods. It also enables histopathological or molecular studies of intact organs after vascular leakage. Thus, this novel IRF method provides a significantly improved technology for *in vivo* proof-of-concept studies where vascular leakage in a potentially important pathogenic factor.

What is known about this topic?

- *In vivo* labelling of albumin with Evans Blue (EB) following its intravenous injection into small mammals is a physiologically relevant approach to study vascular permeability in tissues.
- Current EB methodology using absorbance-based determination of EB was developed in the 1950s and has low sensitivity, inconveniently long experimentation time (several days) and inability to use organs for further studies in current mouse models of vascular permeability.
- Research studying inflammation and vascular permeability in murine models is currently limited by methodology relying on tissue extraction of EB and determination of EB by absorbance.

What does this paper add?

- The paper describes new near-infrared fluorescence (IRF) methodology for *in vivo* studies of albumin-bound EB, which is in several aspects superior to traditional methods.
- IRF methodology is highly sensitive, quantitative, convenient and fast without a need to correct for heme pigments.
- IRF methodology affords immediate results and leaves solid organs intact for histopathology and other desirable analyses. This saves time and number of animals subjected to experimentation.

Acknowledgements

We gratefully acknowledge histopathology analyses performed by Dr. K. Osborne of the University of California at San Diego. A.v.D. was supported by a Research Training Award for Fellows from the American Society of Hematology. L.O.M., W.R. and J.H.G. were supported by grants from the National Institutes of Health (R01HL104165, R01 HL097387, P01HL31950 & R01HL052246)

Conflicts of interest

None disclosed.

References

1. Goldenberg NM, Steinberg BE, Slutsky AS, et al. Broken barriers: a new take on sepsis pathogenesis. Sci Transl Med 2011; 3: 88ps25.
2. Lee WL, Slutsky AS. Sepsis and endothelial permeability. N Engl J Med 2010; 363: 689–691.
3. Russel JA. The current management of septic shock. Minerva Med 2008; 99: 431–458.
4. Caster WO, Simon AB, Armstrong WD. An Evans blue method for the determination of plasma volume in the soft tissues of the rat. J Appl Physiol 1954; 6: 724–726.
5. Caster WO, Simon AB, Armstrong WD. Evans blue space in tissues of the rat. Am J Physiol 1955; 183: 317–321.
6. Caster WO, Garamella JJ, Veleso A, et al. Effect of acute coronary occlusion upon the movement of Evans blue dye into different areas of pig heart muscle. Am Heart J 1958; 56: 658–661.
7. Darrow AL, Fung-Leung WP, Ye RD, et al. Biological consequences of thrombin receptor deficiency in mice. Thromb Haemost 1996; 76: 860–866.
8. Castellino FJ, Liang Z, Volkir SP, et al. Mice with a severe deficiency of the endothelial protein C receptor gene develop, survive, and reproduce normally, and do not present with enhanced arterial thrombosis after challenge. Thromb Haemost 2002; 88: 462–472.
9. Xu Z, Castellino FJ, Ploplis VA. Plasminogen activator inhibitor-1 (PAI-1) is cardioprotective in mice by maintaining microvascular integrity and cardiac architecture. Blood 2010; 115: 2038–2047.
10. Linderkamp O, Mader T, Butenandt O, et al. Plasma volume estimation in severely ill infants and children using a simplified Evans blue method. Eur J Pediatr 1977; 125: 135–141.
11. Finigan JH, Boueiz A, Wilkinson E, et al. Activated protein C protects against ventilator-induced pulmonary capillary leak. Am J Physiol Lung Cell Mol Physiol 2009; 296: L1002-L1011.
12. Ryan AJ, McCoy DM, McGowan SE, et al. Alveolar sphingolipids generated in response to TNF-alpha modifies surfactant biophysical activity. J Appl Physiol 2003; 94: 253–258.
13. Verbrugge SJ, Vazquez de AG, Gommers D, et al. Exogenous surfactant preserves lung function and reduces alveolar Evans blue dye influx in a rat model of ventilation-induced lung injury. Anesthesiology 1998; 89: 467–474.
14. Zhuang J, Xu J, Zhang C, et al. IL-1beta acutely increases pulmonary SP and permeability without associated changes in airway resistance and ventilation in anesthetized rats. Respir Physiol Neurobiol 2011; 175: 12–19.
15. Knezevic N, Tauseef M, Thennes T, et al. The G protein betagamma subunit mediates reannealing of adherens junctions to reverse endothelial permeability increase by thrombin. J Exp Med 2009; 206: 2761–2777.
16. Rice BW, Contag CH. The importance of being red. Nat Biotechnol 2009; 27: 624–625.
17. Kerschen EJ, Fernandez JA, Cooley BC, et al. Endotoxemia and sepsis mortality reduction by non-anticoagulant activated protein C. J Exp Med 2007; 204: 2439–2448.
18. Dallal MM, Chang SW. Evans blue dye in the assessment of permeability-surface are product in perfused rat lungs. J Appl Physiol 1994; 77: 1030–1035.
19. Green TP, Johnson DE, Marchessault RP, et al. Transvascular flux and tissue accrual of Evans blue: effects of endotoxin and histamine. J Lab Clin Med 1988; 111: 173–183.
20. Rogers DF, Boschetto P, Barnes PJ. Plasma exudation. Correlation between Evans blue dye and radiolabeled albumin in guinea pig airways in vivo. J Pharmacol Methods 1989; 21: 309–315.
21. Zuccarello M, Anderson DK. Protective effect of a 21-aminosteroid on the blood-brain barrier following subarachnoid hemorrhage in rats. Stroke 1989; 20: 367–371.
22. Liu W, Hendren J, Qin XJ, et al. Normobaric hyperoxia attenuates early blood-brain barrier disruption by inhibiting MMP-9-mediated occludin degradation in focal cerebral ischemia. J Neurochem 2009; 108: 811–820.
23. Muzumdar RH, Huffman DM, Calvert JW, et al. Acute humanin therapy attenuates myocardial ischemia and reperfusion injury in mice. Arterioscler Thromb Vasc Biol 2010; 30: 1940–1948.